https://ntrs.nasa.gov/search.jsp?R=20180006385 2019-04-29T08:44:22+00:00Z

Optothermal stability of large ULE and Zerodur mirrors

Thomas E. Brooks*[a], Ron Eng[a], H. Philip Stahl[a]
[a] NASA's Marshall Space Flight Center, AL 35812;

ABSTRACT

Marshall Space Flight Center's (MSFC) X-ray and Cryogenic Test Facility (XRCF) has tested the optothermal stability of two low-CTE, large-aperture mirrors in a thermal vacuum chamber. The mirrors deformed from several causes such as: thermal gradients, thermal soaks, coefficient of thermal expansion (CTE) gradients, CTE mismatch, and stiction. This paper focuses on how the aforementioned conditions affected the surface figure of the large optics while in vacuum at temperatures ranging from 230 to 310 K (-43 to 37 ˚C). The presented data, conclusions, and taxonomy are useful for designing mirrors and support structures for telescopes. The data is particularly useful for telescopes that require extreme dimensional stability or telescopes that operate at a temperature far from ambient.

Keywords: CTE homogeneity, mirror, thermal soak, thermal expansion, surface figure error, finite element analysis, CTE

1. INTRODUCTION

Thermal effects degrade optical wavefront. There are several kinds of thermal effects and many ways in which they degrade the optical system. This paper focuses on the effect that thermal gradients and thermal soaks have upon the surface figure of a mirror and the design features that make the effects manifest themselves. Several large-aperture optics have been tested in the XRCF, including James Webb Space Telescope's (JWST) flight mirrors. Many more large-aperture optics will be tested in the coming years. This paper includes data from the tests done on a 1.5m Ultra-Low Expansion (ULE) mirror, and a 1.2m Zerodur mirror. The results of the conducted tests are summarized in the top two rows of the table below. Mirrors that were previously tested in the XRCF in a similar manner are also included in the table.

Table 1: Overview of Tested Mirrors

Material	Measured Aperture (m)	Mirror Diameter (m)	Mirror Thickness at mirror ID/OD (m)	Change in RMS Surface per change in Temperature from CTE gradients (nm / ˚C)	Areal Density (kg/m^2)
Zerodur	1.06	1.2	0.071/0.124	0.17†	40
ULE	1.34	1.45	0.173/0.176	0.27†	50
"CERAFORM" SiC	0.51	0.51	0.059	0.23*	22
"SuperSiC" SiC	0.25	0.25	0.035	0.105ǂ	22

† Sensitivity estimated with a soak between 293 and 230K see Figure 8 and Figure 22
* Sensitivity estimated with a soak between 293 and 150K[1]
ǂ Sensitivity estimated with a soak between 293 and 196K[1]

2. TEST SETUP AND DATA FORMAT

The two tested mirrors were spherical mirrors whose surfaces were measured interferometrically using a center of curvature test as shown in Figure 1. Surface measurements were taken while the mirror assembly was isothermal at room temperature and these surfaces were subtracted from perturbed surface measurements to determine the effect of the thermal soak and thermal gradients. To be explicit, a thermal soak test follows the steps enumerated below:

1) A mirror rests inside of an isothermal environment for an extended period of time.
2) When the mirror becomes isothermal, the initial surface figure measurement is taken.
3) The environment around the mirror is changed to a new isothermal temperature state.
4) The mirror soaks in this new environment until it reaches isothermality at the environment's temperature.
5) A surface figure measurement is taken of the mirror (the perturbed surface figure measurement).
6) Perturbed surface figure measurements are taken for isothermal states at several temperatures.
7) Steps 1-6 are repeated for several cycles.

*thomas.brooks@nasa.gov; (256)544-5596 nasa.gov
2018 SPIE Optical Engineering + Applications (OP180); Paper 10743-9

The thermal gradient test gives insight into the mirror's sensitivity to thermal gradients by following a procedure which is similar to the thermal soak test and is enumerated below:

1) A mirror rests inside of an isothermal environment for an extended period of time.
2) When the mirror becomes isothermal, the initial surface figure measurement is taken.
3) Heat lamps beside the mirror are turned on to induce a lateral thermal gradient.
4) The mirror soaks in this new environment until the mirror's surface changes by approximately the test repeatability over the course of an hour.
5) A surface figure measurement is taken of the mirror in its perturbed state (the perturbed surface figure measurement).
6) Perturbed surface figure measurements are taken for steady states at several heat lamp power levels.

Delta maps are created by subtracting an ambient surface figure measurement from each of the perturbed surface figures. The delta maps show how much the mirror's figure has changed due to the change in the mirror and mount's temperature. The delta maps' shape and root-mean-square (RMS) are used to quantify the impact of thermal gradients and thermal soaks on the mirror's surface figure.

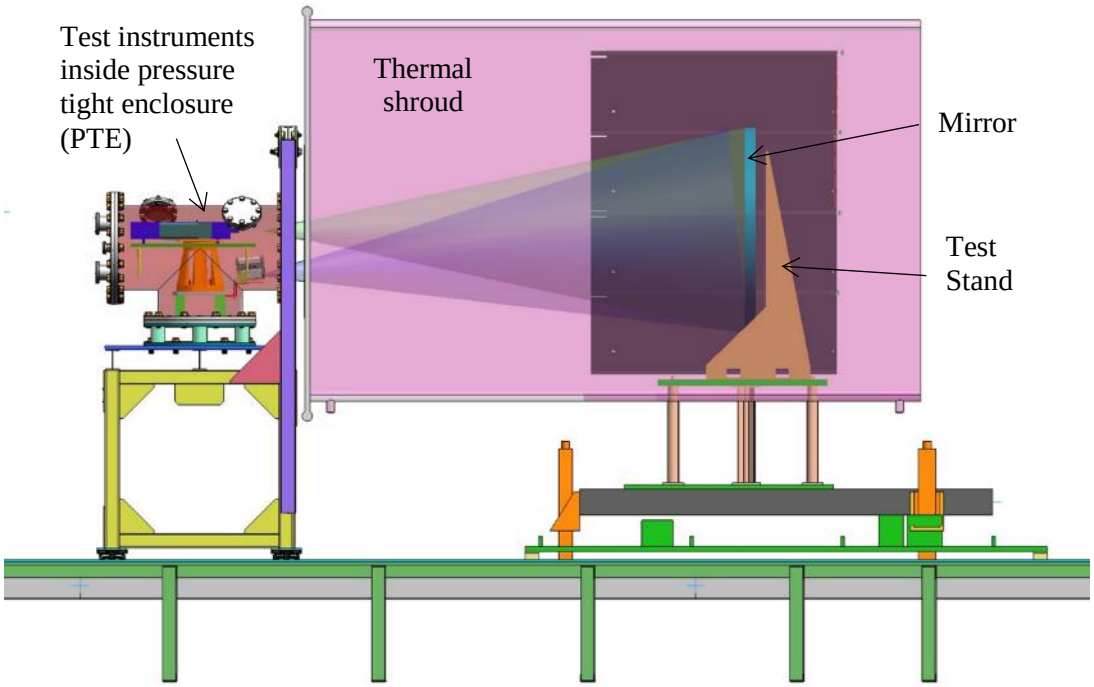

Figure 1: Test Setup: The mirror sits inside of the XRCF's large vacuum chamber, and it is supported by a kinematic hexapod mount. The back structure kinematically mounts to the test stand using cone-vee-flat blocks and tooling balls. An interferometer is placed at the mirror's center of curvature and the surface figure error of the mirror is measured. An infrared camera is used to measure the thermal emission of the mirror's front face, and this data can be processed to gain an indirect measurement of the mirror's temperature distribution. Thermal diodes are located on the mirror and its mount to ensure that the mirror is isothermal at every SFE measurement.

3. CORRELATION OF MODEL TO TEST DATA

Neither mirror has a known CTE distribution. However, there are many literary resources that provide an expectation for the range of possible CTE distributions of Zerodur.[2][3] The ULE mirror was made using an experimental process which included a thermal soak that occurred at such an elevated temperature as to potentially substantially change the CTE of the mirror, so its CTE distribution is not well bounded by historical data. Because the CTE distributions are unknown, a correlation process has been used to correlate the thermoelastic model to the test data by tuning the CTE distribution. This process is used to correlate models of both mirrors to their test data.

3.1 Test Data Filtering Process

Interferometric shearing is clearly apparent in the delta map shown in Figure 2. Some small fraction of the interferometer's many pixels are biased and measure surface heights that are significantly different than the rest of the pixels. This interferometric shearing is caused by the mirror moving relative to the interferometer, so when the delta map is taken, the erroneous pixels appear to move on the mirror's surface and do not cancel themselves out during subtraction. It can be seen in Figure 2 as very high surface measurement circles (red) above very low surface measurement circles (blue). This error source should not be modeled, so it is simply removed by filtering. Unfortunately, many of the erroneous measurements caused by this interferometric shearing do not exceed the bounds of truly measured surface figure errors, so they cannot be filtered out by putting maximum and minimum bounds on the measurement. A gradient method is used to filter the measurement instead of a range filtering technique. The gradient filtering technique is described graphically in Figure 2. A comparison between the original, unfiltered 230K delta map and the filtered 230K delta map is shown in Figure 3.

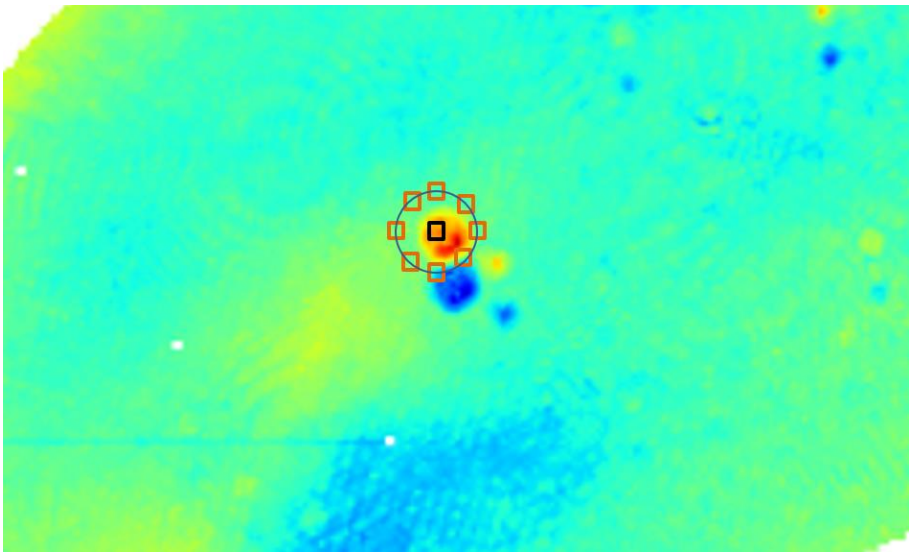

Figure 2: Filtering Example. The black pixel is being tested for filtering, and the difference between the orange and black pixels' values are found. If the difference between the black pixel's value and the orange pixels' values is too great for half or more of the pixel differences, then the black pixel is filtered out. The distance between the black square and every orange square is the same, so the difference in the surface measured at black and orange pixels is effectively a SFE gradient.

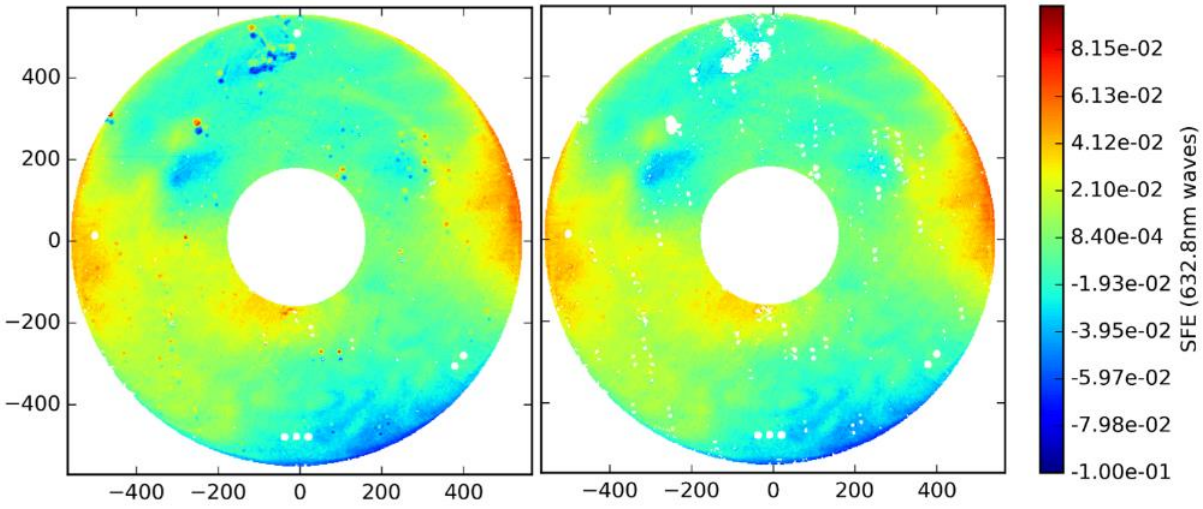

Figure 3: Comparison between filtered and unfiltered test data from the Zerodur test. The left figure shows a raw 292-230K delta map without filtering. The right image shows what the data looks like after filtering is performed.

3.2 Mathematical Process

In brief: the RMS of the difference between the test data and analysis results is minimized by changing the CTE distribution of the mirror within reasonable bounds.

This is accomplished using the following steps:

1) Apply a CTE distribution to the mirror. The CTE distributions for this work were a summation of Zernike shapes with variation from case to case resulting from an intentional variation in the Zernike coefficients. For the Zerodur mirror, Zernike shapes were used between standard Zernike number 4 and 91 (from n=2, m=0 to n=12, m=12). This process is described mathematically in equation (1) and graphically in Figure 4. For the ULE mirror, a similar process was used but each section of the mirror was given a unique CTE distribution because the mirror was made by combining several different boules together using low temperature fusion (LTF).
2) Run the mirror finite element model (FEM) through NASTRAN.
3) Run the displacements found with NASTRAN through SigFit to find the SFE after power and rigid body motions have been removed.
4) Subtract the analysis' surface figure error from the measured surface figure error to find the residual SFE.
5) RMS the residual SFE.
6) Calculate the objective function by combining the RMS residual SFE with a term that constrains the CTE distribution's P-V to a realistic number.
7) Repeat steps 1-6 until the objective function reaches a minimum.

Producing a CTE distribution is central to these steps. Mathematically, this is described by equation (1).

$$[\alpha_{x,y}] = \sum_{n=2}^{12} \sum_{m=0}^{n} C_{n,m}[U_{n,m}] \tag{1}$$

Where $\alpha_{x,y}$ is the CTE distribution, $C_{n,m}$ is the coefficient for the Zernike shape which is represented with $U_{n,m}$. This summation is expressed graphical in Figure 4.

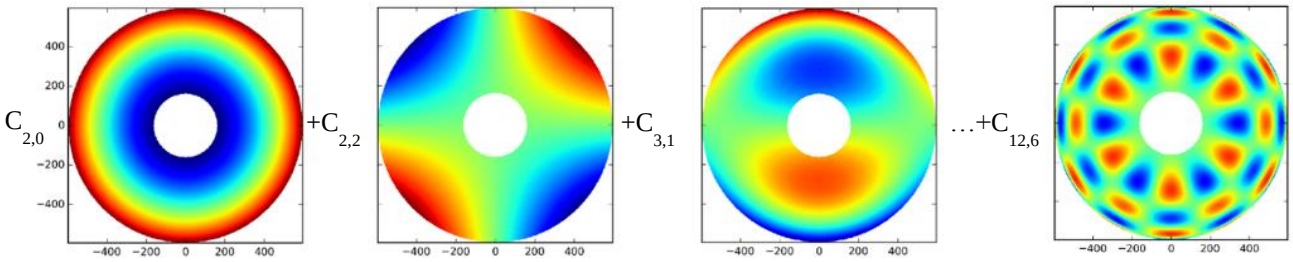

Figure 4: This figure shows a few of the Zernike shapes that are summed in the summation process which is mathematically described by equation (1). The coefficients ($C_{n,m}$) are multiplied with the Zernike shapes, and the resulting surfaces are summed to create a CTE map like what is shown in Figure 5.

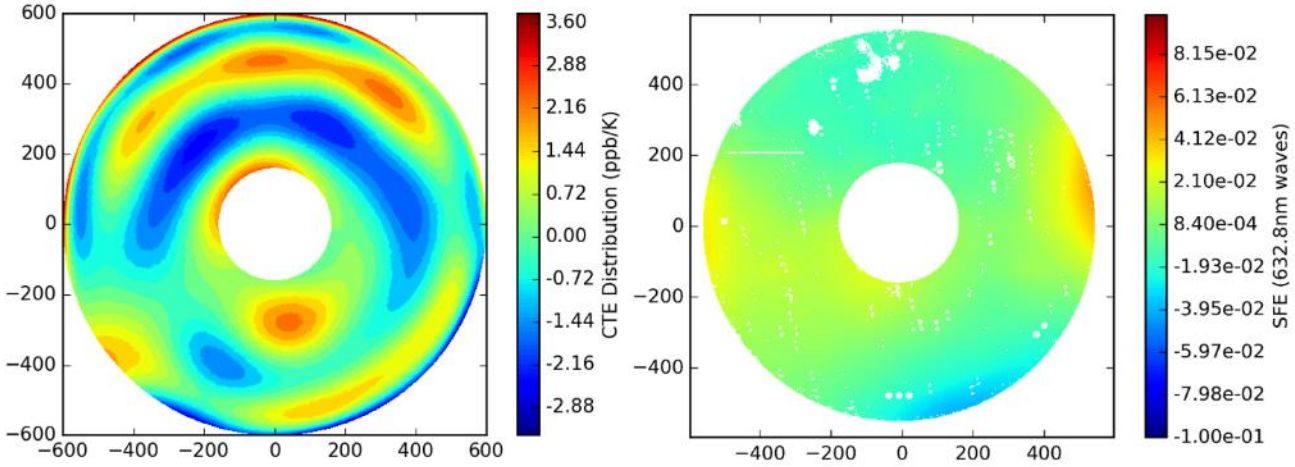

Figure 5: Left: A CTE distribution that was produced using the correlation process. Right: The SFE that this CTE distribution causes when the mirror's temperature decreases by 62 degC and is filtered at the same points as the test data.

4. ZERODUR MIRROR TEST

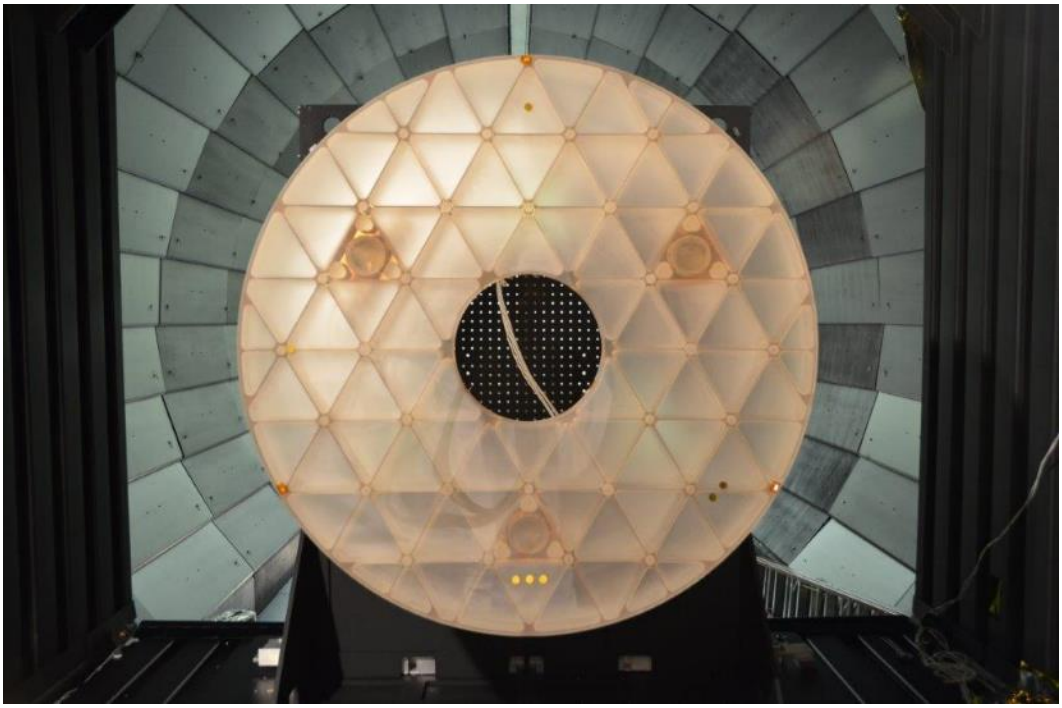

Figure 6: The ELZM is shown (from the interferometer's perspective) mounted in the XRCF's large cryogenic chamber.

4.1 Thermal soak test data

Temperature measurements were taken continuously at 21 locations on the mirror throughout the test. Most of the diode locations are in Figure 7. The mirror's average temperature, maximum temperature, minimum temperature, and temperature gradient are graphed versus time in Figure 8. Vertical blue lines indicate the times at which the surface was measured. The SFE measured at 230K, 250K, and 275K was subtracted by the SFE measured at room temperature to result in the "delta maps" shown in Figure 9. Thermal expansion of the mirror's mount and realignment of the interferometer

resulted in interferometric shearing which is most evident in the 230K and 250K delta maps. The interferometric shearing has been filtered out using a process described in section 3.1.

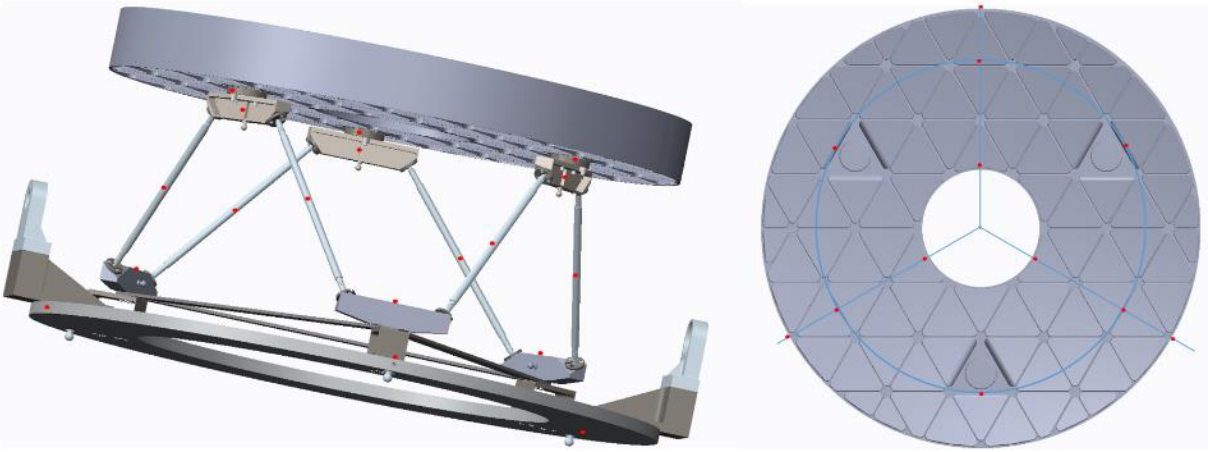

Figure 7: Location of thermal diodes on the mirror and the mount. Not all diodes are visible in this image. In total, 40 diodes measure temperatures on the mirror and mount.

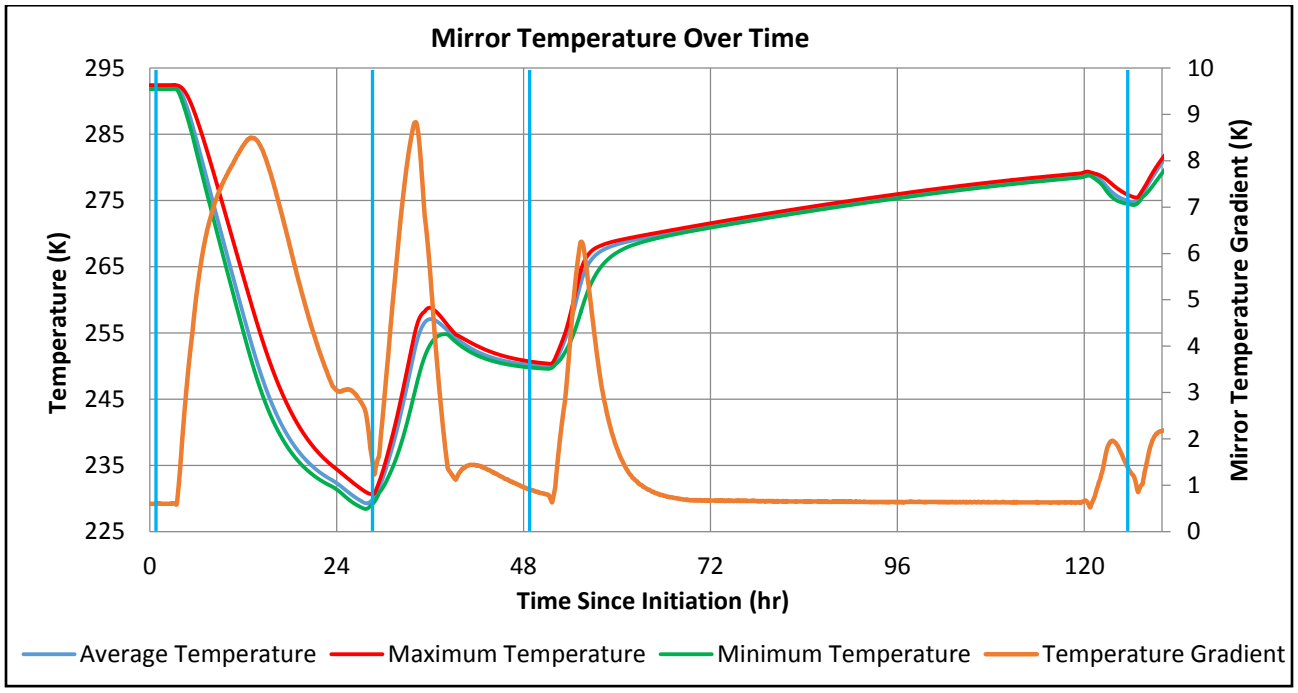

Figure 8: Temperature Data over One Cycle. The left axis indicates the mirror's maximum, minimum, and average temperatures. The right axis indicates the maximum minus the minimum temperature (commonly called a temperature gradient). A small bias between thermocouples puts an artificial floor on the temperature gradient. The vertical, light blue lines indicate the times at which the mirror's surface figure is measured.

The peak to valley (P-V) of the mirror's temperature distribution is very small at every SFE measurement with the least isothermal measurement occurring at the 230K where there is a 1.5K temperature gradient in the mirror (with a 1K gradient floor). Analysis indicates that such a small temperature gradient will have a negligible impact on the mirror's SFE because of the thermal gradient's shape and the low average CTE of the mirror. Therefore, most of the measured SFE is being caused by CTE gradients.

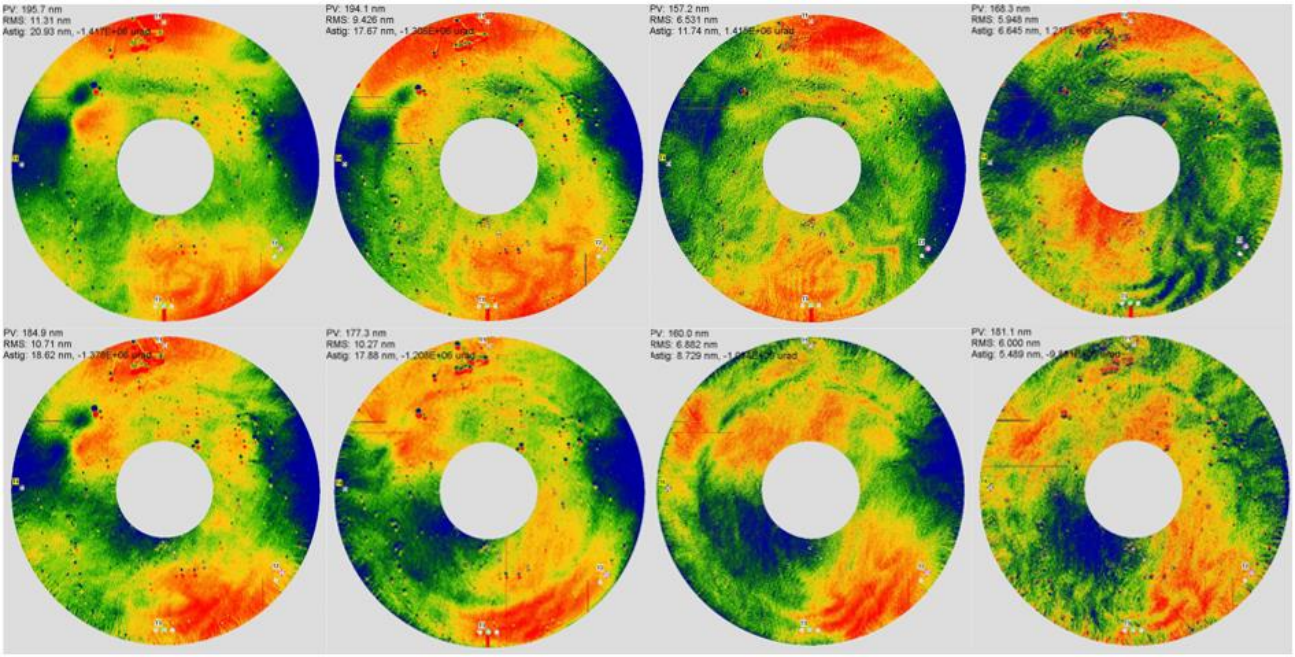

Figure 9: Delta maps for cycles one and two. The first cycle is on the top row and the second cycle is on the bottom row. The delta maps are (from left to right): 230K-ambient, 250K-ambient, 275K-ambient, and final ambient - initial ambient.

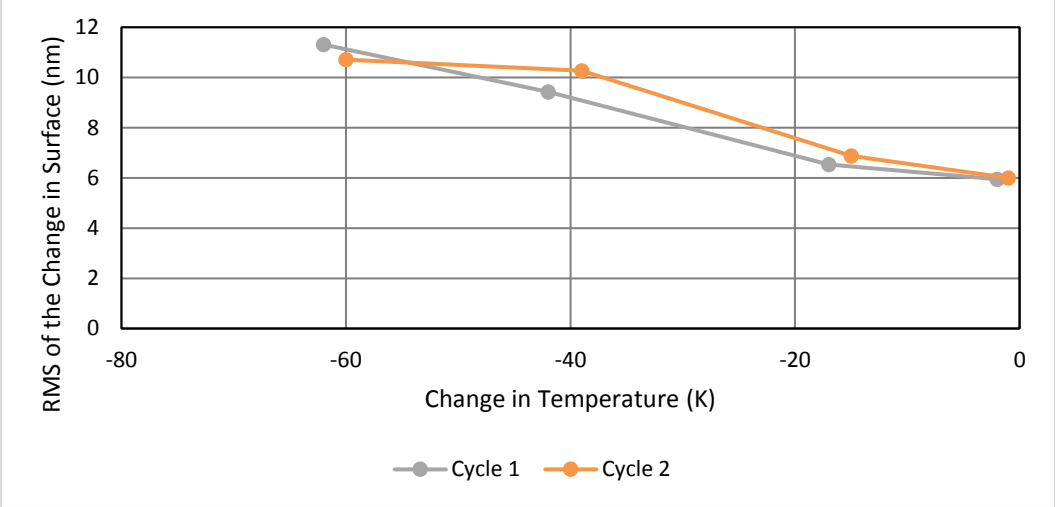

Figure 10: This graph plots the RMS of the delta map for each cycle versus the change in temperature. The data indicates that the mirror's surface changes by 0.17 nm RMS per degree temperature change.

4.2 Modeling results

A finite element model (FEM) was made of the mirror and mount using NASTRAN. Images of this FEM are in Figure 11. The displacements from the NASTRAN analysis were input into a SigFit analysis to determine the mirror's SFE (with defocus removed). Defocus was removed, because the interferometer is put into focus to take the measurement. Initial analyses included both the mirror and the mount and concluded that the mount's effect on the mirror's SFE was relatively

small. Analysis was done to determine the magnitude of the effect of thermal gradients. Temperature measurements, thermal analysis, and structural analysis culminated in the conclusion that thermal gradients did not have a sizeable effect on the mirror's SFE. The isothermal test conditions made temperature gradients of little importance even though thermal gradients are often more important than CTE gradients during operation of a telescope.

The CTE distribution of the mirror was not known in advance, so several CTE distributions were placed on the mirror to bound the effect. Schott provides an example CTE distribution in their catalogue and that distribution is shown in Figure 12.[2]

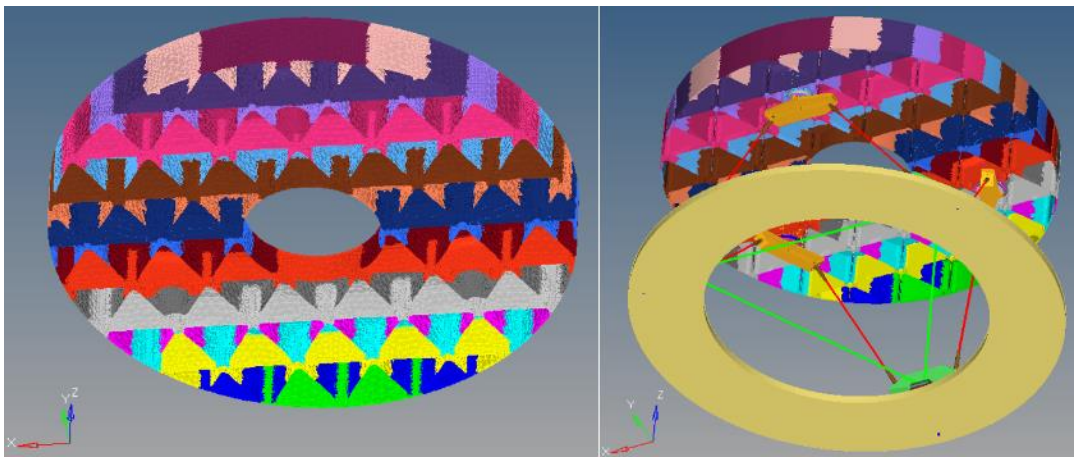

Figure 11: Left: An image of the FEM is shown with all things hidden except the mirror. The mirror has a lateral (tip/tilt) CTE distribution. Right: An image of the FEM is shown that includes the mount.

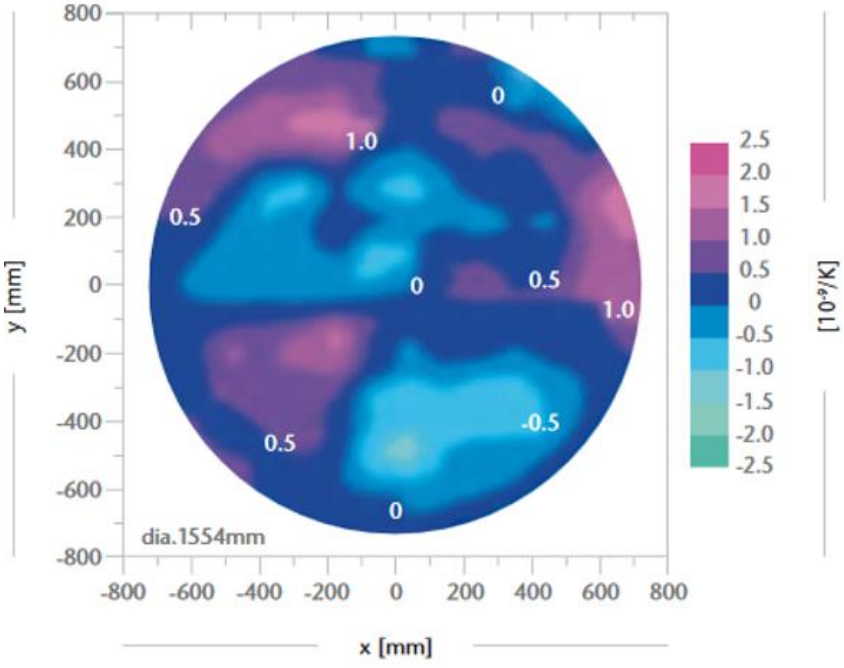

Figure 12: This is the CTE homogeneity of a sample Zerodur boule.[2]

This distribution appears to have very low order spatial terms like astigmatism and coma, so code was written to produce CTE distributions of similar shapes. The P-V of the CTE distribution was limited to 5ppb/K to be in line with data in Figure 13 that is from a paper published by Schott.[3] These efforts resulted in a prediction that matched the measured data's RMS quite well as shown in Figures Figure 14, Figure 15, and Figure 16.

	Dimension	Number of Samples	CTE (0°; 50°) absolute value [ppb / K]		CTE (0°; 50°) homogeneity [ppb / K]	
Year	[mm]	#	Specification	Achieved	Specification	Achieved
2003	4100 x 171	18	+/- 50	66	20	18[1]
2005	3610 x 370	12	+/- 100	80	30	25[1]
2009	3700 x 163	36	+/- 150	54	40	9
2010	3400 x 180	12	+/- 100	42	30	5
2012	4250 x 350	16	+/- 30	60	40	5
2014	4250 x 350	16	+/- 30	0	40	3
2016	4060 x 103	16	+/- 50	36	20	7
2016[2]	4000 x 100	12	+/- 150	15	20	4

Figure 13: This is an image of a table from a paper published by Schott.[3] The first two measurements (circled in red) were taken using an old dilatometer setup. The newer, more accurate measurements indicate much better homogeneity which is clustered around 5ppb/K.

Several CTE distributions were produced that resulted in SFEs that closely matched the test data. Multiple CTE distributions cause the same SFE from a thermal soak. This is possible because some CTE shapes have a small impact on SFE, so the CTE distribution may change by a large amount without impacting SFE by more than the SFE measurement accuracy.[4]

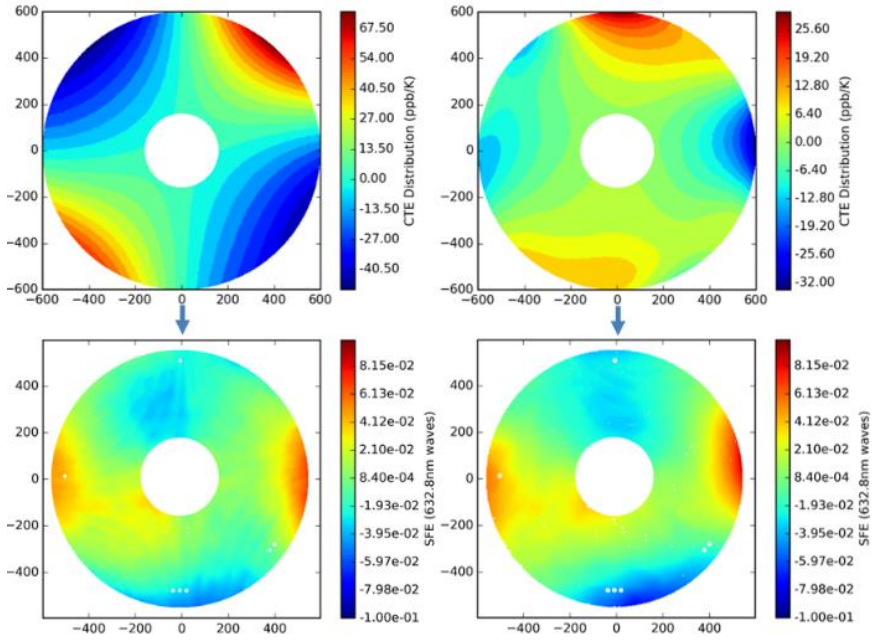

Figure 14: The top row shows the CTE distributions that result in the SFEs shown on the bottom row. The top left CTE distribution has a P-V of 110 ppb/K. The top right CTE distribution has a P-V of 60 ppb/K. Even though the CTE distributions' P-Vs are quite different in magnitude, the SFEs that result from these CTE distributions (and a -62 ˚C change in temperature) are similar as is seen in the bottom row. This is because a first order astigmatism CTE distribution does not greatly affect SFE.[4]

The two CTE distributions shown in Figure 14 are unrealistic, because their P-V is significantly greater than what Schott has measured before. Therefore, a penalty was added to the correlation process's objective function for unrealistic CTE distributions, and the correlation algorithm resulted in the CTE distributions and SFEs shown in Figure 15 and Figure 16. The two CTE distributions match the measured SFE to within the repeatability of the SFE measurements. Both CTE distributions have reasonable P-Vs (7ppb/K and 3ppb/K), so they are both considered to be successful correlations.

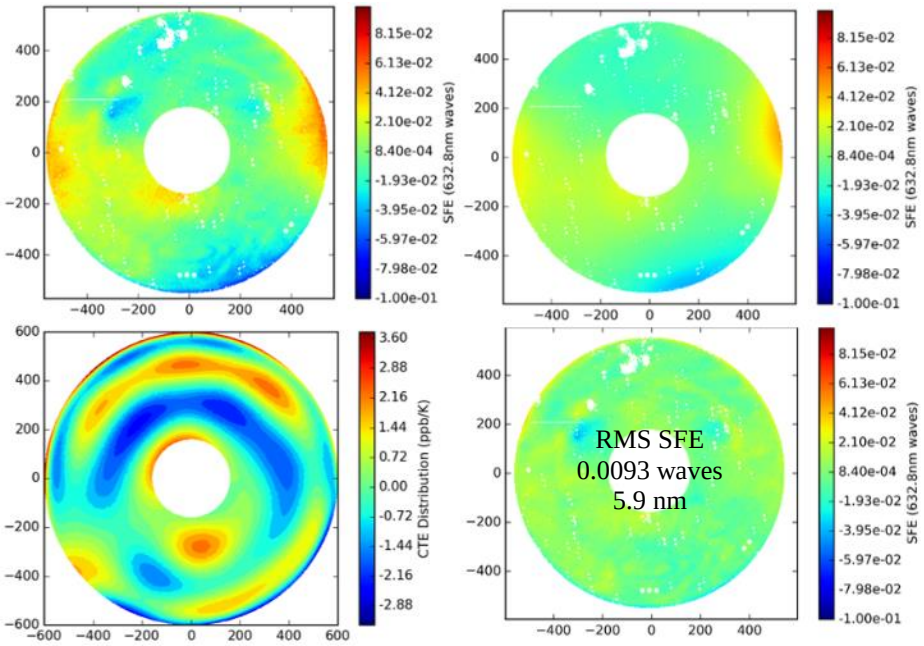

Figure 15: Correlation Results. The top left image shows the filtered, measured SFE for a 292K-230K soak. The top right image shows the filtered, analytical SFE for a 292K-230K soak. The bottom left image shows the CTE distribution that was used to obtain the analytical SFE. It has a P-V of roughly 7 ppb/K which is within the range of measured CTE distributions shown in Figure 12. The bottom right image shows the difference between the measured and analytical SFE. The RMS of the difference between the measured and analytical SFE is 5.9nm which is better than the repeatability of the test, so the correlation process is considered to be successfully completed.

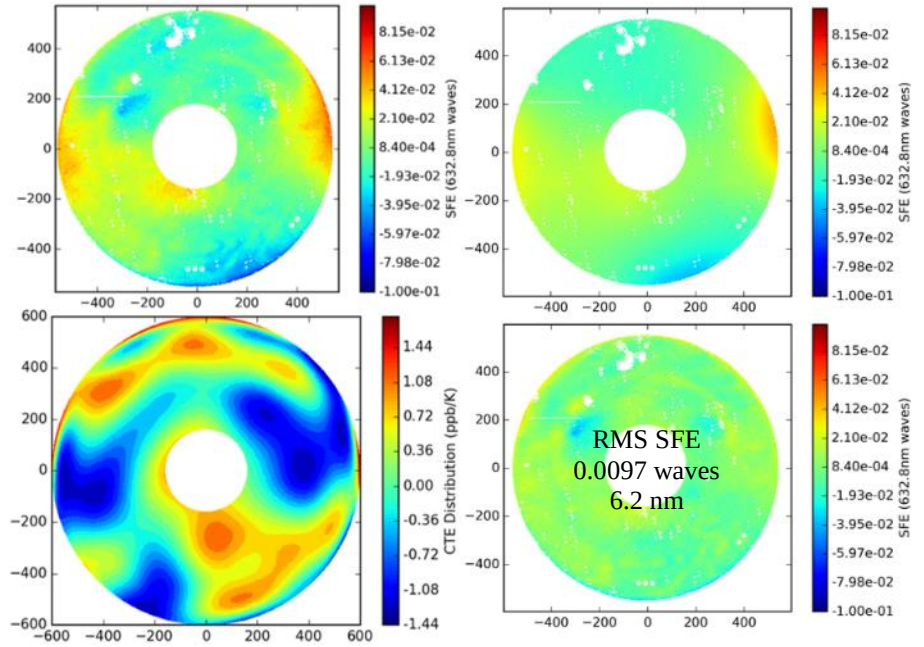

Figure 16: Correlation Results. The images are in the same order as is shown in Figure 15. The CTE distributions have some similarities, yet they are distinctly different and still result in similar SFE maps. This CTE distribution has a P-V of 3ppb/K which is within the range of measured CTE distributions shown in Figure 13.

5. ULE MIRROR TEST

5.1 Thermal soak test and model data

Temperature measurements were taken continuously at 30 locations on the mirror throughout the test. Some of the diode locations may be seen in Figure 17. The mirror's average temperature and temperature gradient are graphed versus time in Figure 19. The SFE measured at 230K, 250K, and 275K was subtracted by the SFE measured at room temperature to result in the "delta maps" shown in Figure 20. Thermal expansion of the mirror's mount and realignment of the interferometer resulted in interferometric shearing which is most evident in the 230K and 250K delta maps. The interferometric shearing has been filtered out using a process described in section 3.1.

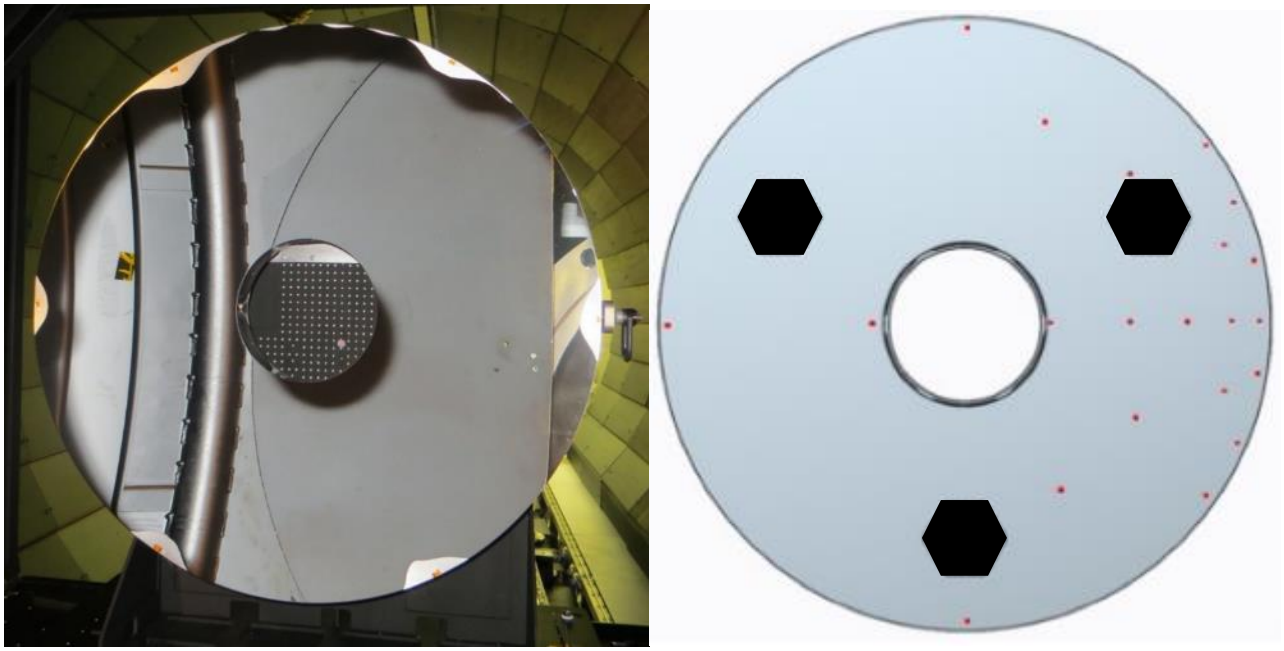

Figure 17: Left: Image of the mirror inside of the XRCF. Right: Image of the back of the mirror with the diode placements shown. Not all diodes are visible in this image. In total, 39 diodes measure temperatures on the mirror (30) and mount (9).

The six petals exist on the edge of the mirror's surface (see Figure 17) due to the experimental process used to produce the mirror. The mirror's surface was masked down to an aperture of 1.34m to avoid those petals, so all surface figure plots are actually for 1.34m of the mirror.

A comparison between the ambient surface figure measurement at the start of the first thermal cycle and the ambient measurement at the start of the second thermal cycle showed a large hysteresis which is shown in Figure 18. This caused the performance of three thermal cycles in order to obtain two consistent, back-to-back thermal cycles. The hysteresis was explained by a stiction-slip event between two of the ribs in the mirror's internal structure. This stiction-slip event renders the first cycle's surface figure measurements nearly useless, because any delta maps obtained relative to the first cycle's measurements will contain the hysteresis which is entirely the result of the experimental process used to make the mirror and of little importance for characterizing the CTE homogeneity.

Temperature data for all three thermal cycles is shown in Figure 19. The mirror is soaked at 292-230-250-275K during each thermal cycle. The peak-to-valley of the mirror's temperature is shown in this graph as well. Surface figure measurements were taken immediately before the XRCF's temperature shifted to the next set point.

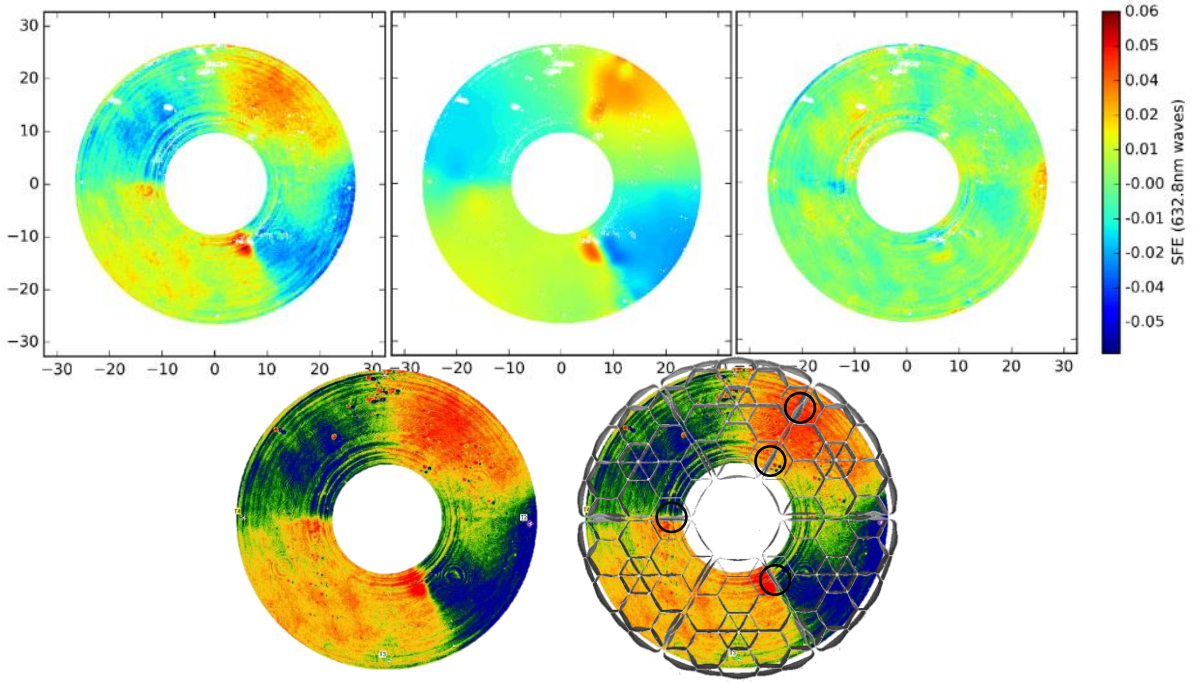

Figure 18: Top Left: Measured hysteresis between thermal cycle 1 and 2 (10.8nm RMS). Top Middle: Analysis that includes potential stiction forces between contacting ribs in the mirror (9.4nm RMS). Top Right: The difference between the measured hysteresis and analysis of stiction forces (5.2nm RMS). Bottom: Buckled ribs superimposed over the measured surface with black circles showing where the computed tomography scan could not detect a gap between the ribs.

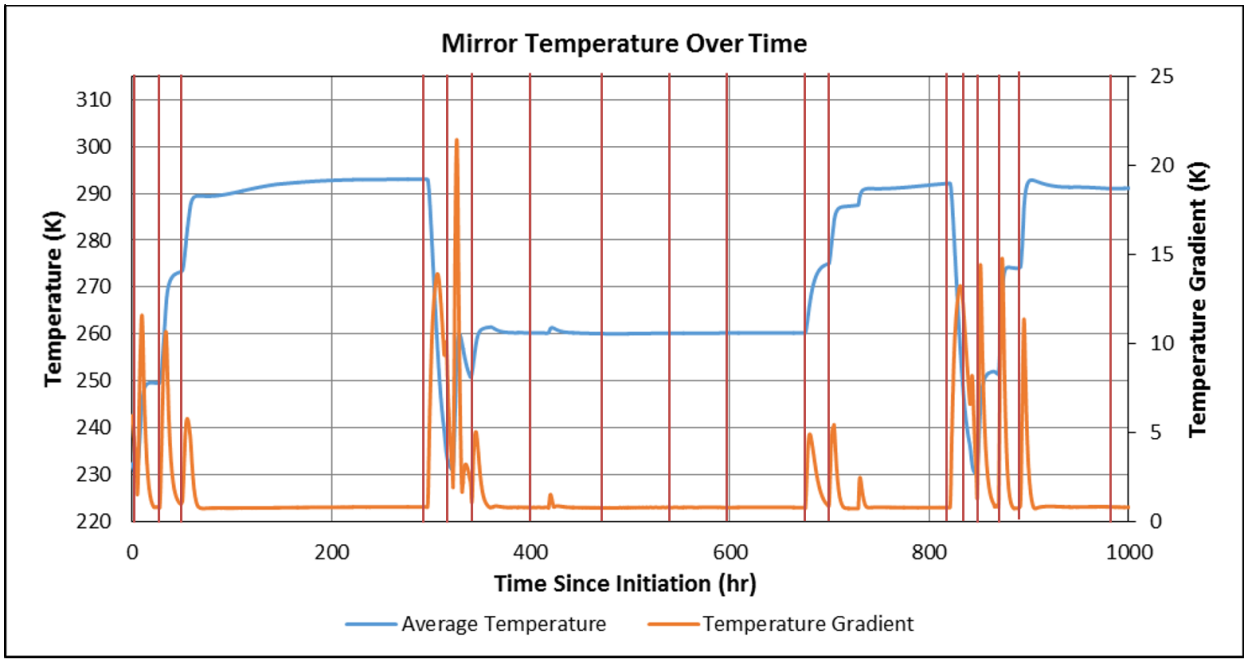

Figure 19: Temperature data over three cycles. The left axis indicates the mirror's average temperature. The right axis indicates the maximum minus the minimum temperature (commonly called a temperature gradient). A small bias between

thermocouples puts an artificial floor on the temperature gradient. The surface figure measurements occurred at the vertical orange lines. These times correspond to the troughs in the temperature gradient.

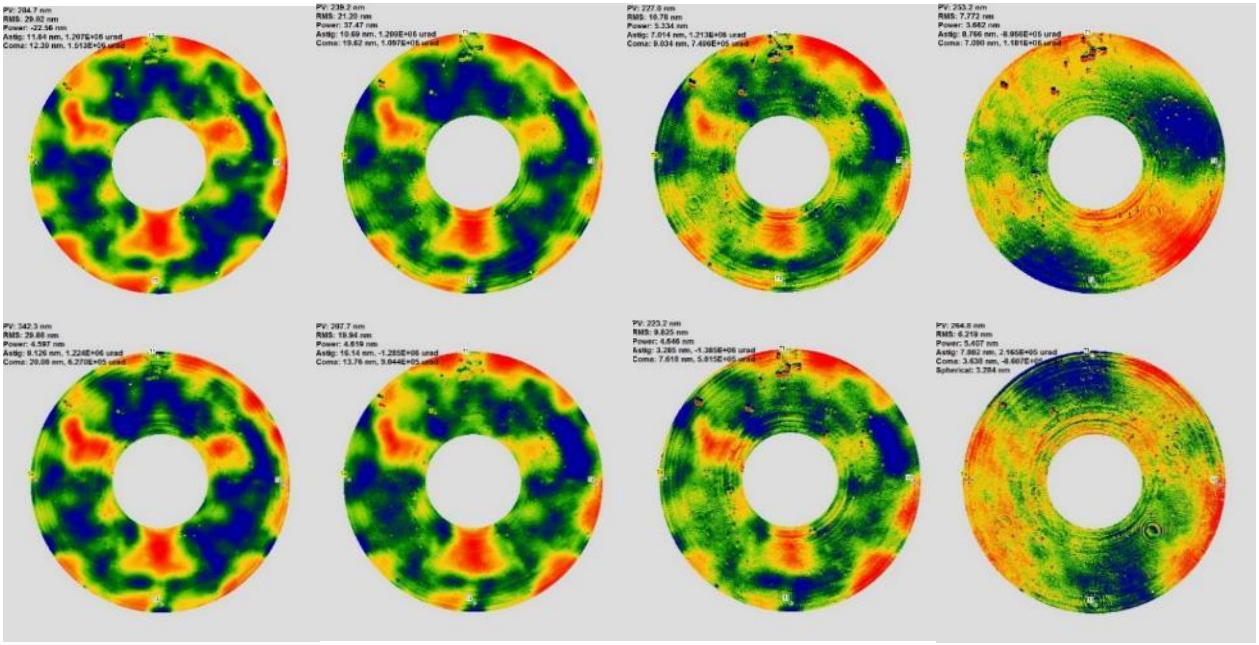

Figure 20: Delta maps for cycles two and three. The second cycle is on the top and the third cycle is on the bottom. The delta maps are (from left to right): 230K-ambient, 250K-ambient, 275K-ambient, and final ambient – initial ambient.

The measurement's reproducibility for each thermal cycle is obtained by comparing ambient measurements at the start and end of the thermal cycle. These delta maps are shown in the fourth column of Figure 20. The reproducibility during cycles two (7.8 nm RMS) and three (6.2 nm RMS) is much improved over the reproducibility during cycle one (11.2 nm RMS). The shapes and amplitudes of the change in surface due to thermal soaks are consistent between cycle two and cycle three as can be seen by comparing Figure 20's top and bottom rows.

Figure 21 shows the sensitivity of this ULE mirror and its mount to thermal soaks by graphing the RMS of the delta map versus the change in temperature that causes the delta map. After the graph surpasses the noise floor of the measurement, the RMS change in surface increases by roughly 0.48nm per degree. In other words, if the mirror and mount were to change by 1 degree, a 0.48nm change in surface is expected. This is a small amount for almost all optical systems, but some systems, like those employing a coronagraph, require extreme wavefront stability which makes this seemingly small perturbation relevant.

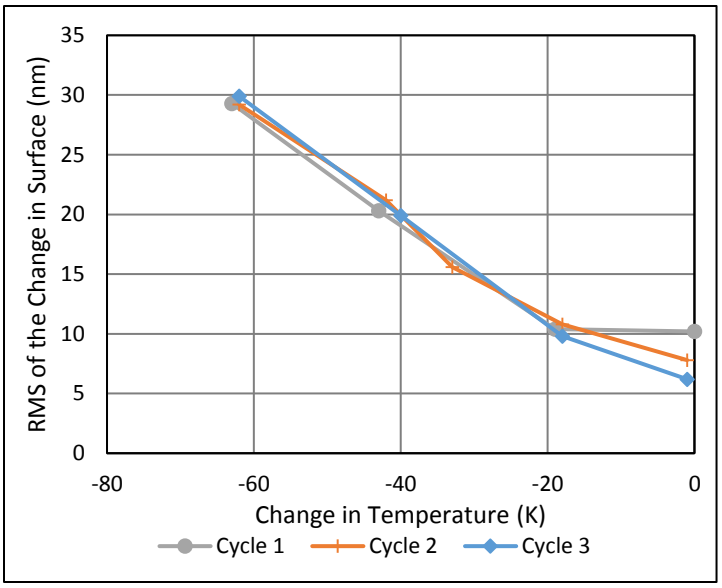

Figure 21: This graph plots the RMS of the delta map for each cycle versus the change in temperature. The slope of the curve is approximately 0.48 nm per degree temperature change. Note that this number includes mount and backplane effects that can be removed by design.

Delta maps are used to understand the change in the mirror's surface due to the change in the mirror's thermal state. Unfortunately, the delta maps made evident that the change in the mirror's surface was not entirely due to CTE inhomogeneity as shown in Figure 20. Some

mount effects are present as well (the trefoil aligns with the bond pads), and an effort has been made to remove the mount effects, so that the effect of CTE inhomogeneity can be seen.

An analysis correlation process resulted in estimates of the mount and inhomogeneity effects shown in Figure 22. A 62 K change in the mirrors temperature resulted in a 16.6nm change in the mirror's surface due to inhomogeneity effects. Therefore, the mirror produces 0.27 nm RMS of SFE per degree change in temperature because of CTE inhomogeneity effects. The inhomogeneity effects exhibit mid-spatial frequency errors in ULE and low spatial frequency errors in Zerodur. Coronagraphs are more sensitive to higher spatial frequency instabilities.

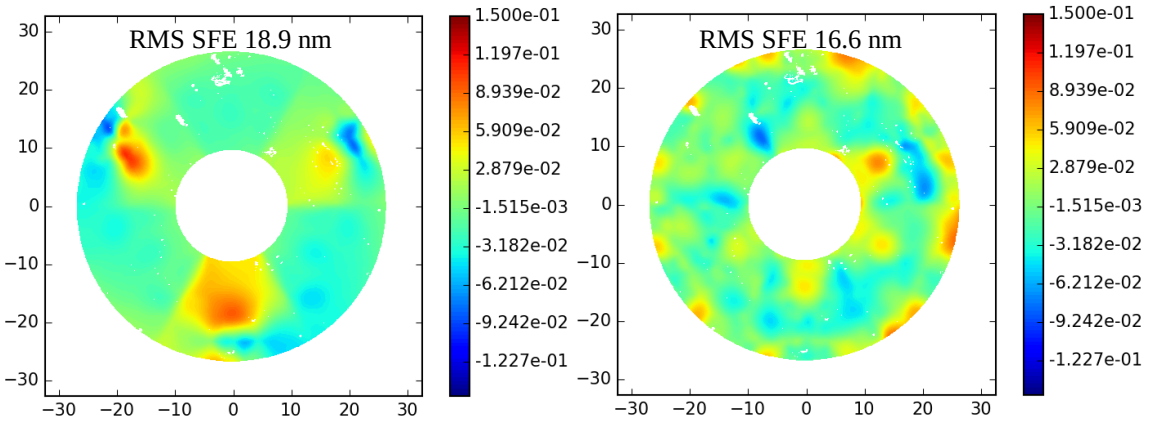

Figure 22: Left: Surface change attributed to mount effects in the ULE thermal soak test. Right: Surface change attributed to inhomogeneity effects in the ULE soak test.

5.2 Thermal gradient test and model data

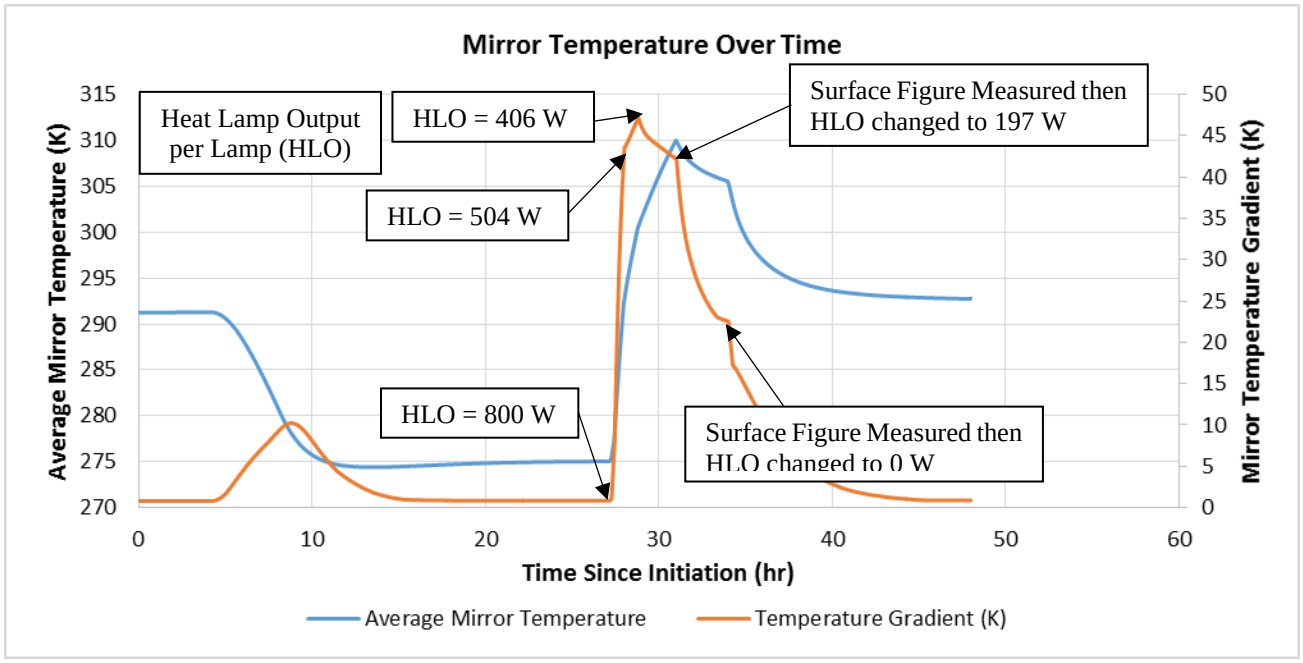

Figure 23: Average mirror temperature and mirror temperature gradient during the thermal gradient test.

The mirror was taken to an isothermal 275K state and its surface was measured. The heat lamp array was turned on and the surface figure was monitored throughout the test. The system was considered to have reached a steady state when its surface had not changed by appreciably more than the repeatability of the surface figure measurement over the past hour.

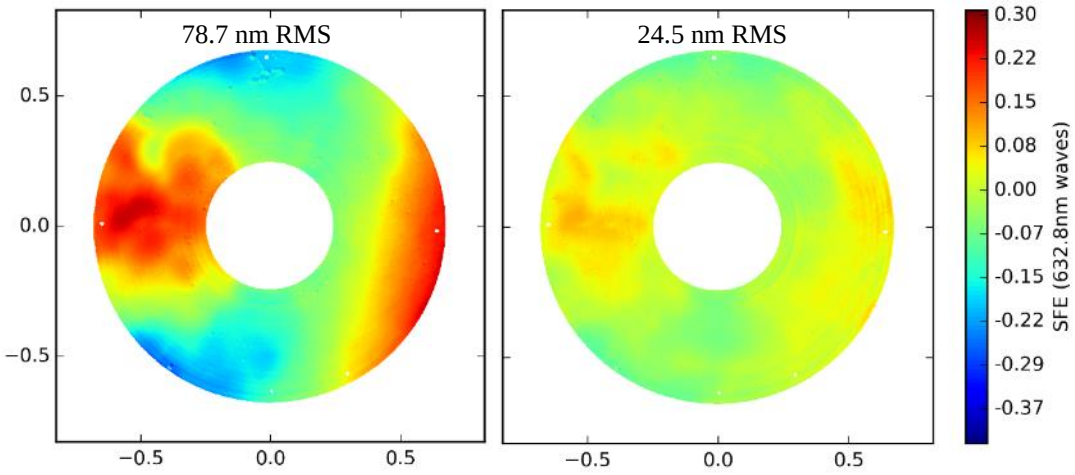

Figure 24: Left: Surface with heat lamps outputting 406W minus surface at isothermal 275K. Right: Surface with heat lamps outputting 197W minus surface at isothermal 275K.

Surface figure measurements were taken at the end of the 406W and 197W dwells. The change in surface figure due to the heat lamps is shown in Figure 24.

A thermal model was made of the test setup and used to estimate the full temperature distribution of the mirror using the measured temperature data. The full temperature distribution was then put into a structural model to calculate thermoelastic deformations and these deformations were used to calculate surface figure error (SFE). The full temperature distribution that was calculated using the thermal model is shown in Figure 25.

ULE can be processed to have a CTE of 0 ± 30 ppb/K at room temperature, but the construction process for this mirror involved elevating the mirror's temperature for an extended period of time after Corning's typical process. Elevating the mirror's temperature may have caused a CTE shift. In order for the model to most closely match the test data, the CTE of the ULE was set to 81ppb/K.

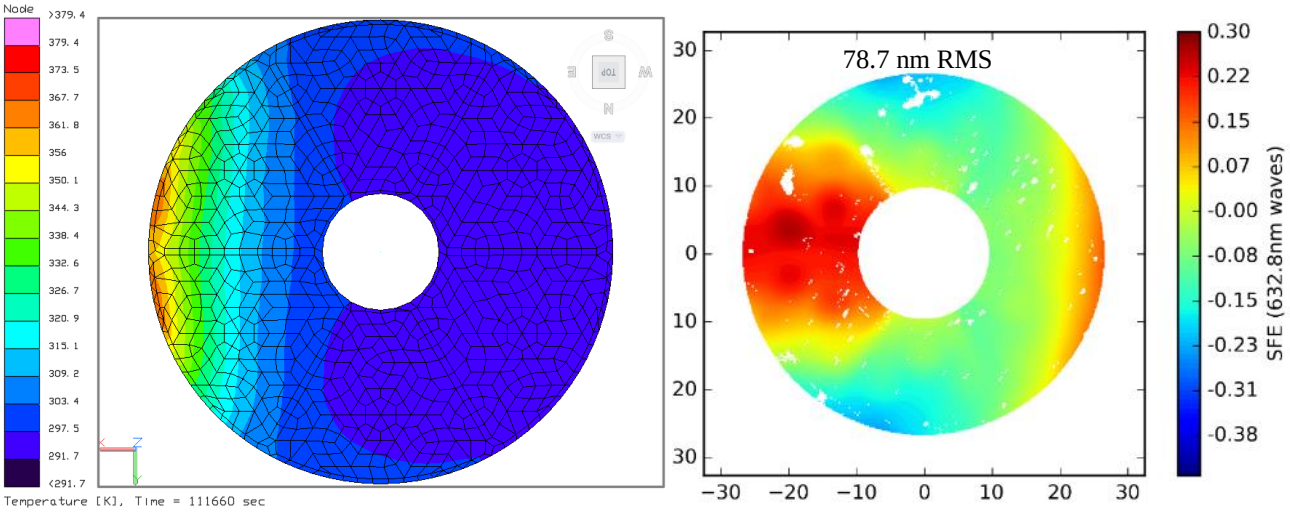

Figure 25: Left: The temperature distribution (ΔT = 87.7 K peak-to-valley) calculated by Thermal Desktop with heat lamps outputting 406W. Right: The surface figure error (RMS = 78.5nm) caused by the temperature distribution and a substrate whose CTE is 81ppb/K on average.

6. CONCLUSION

Optothermal tests have been performed and models have been used to decompose the composite surface figure error into specific thermal effects. Several thermal effects were observed during the test caused by: 1) CTE gradients in the mirror, 2) temperature gradients in the mirror, 3) stick-slip between ribs in the ULE mirror, and 4) CTE mismatch between the mirror and its mount.

Mirrors will bend as their temperature changes, because no material has a perfectly homogeneous CTE. The sensitivity of surface figure to changing temperatures has been found for a 1.45m ULE and 1.2m Zerodur mirror. The 1.45m ULE mirror's surface changed by 0.27 RMS nm per ˚C (excluding power) and the 1.2m Zerodur mirror changed by 0.17 RMS nm per ˚C (excluding power) due to CTE gradients. The ULE mirror was constructed using an experimental process and ULE mirrors that are constructed differently could be less sensitive to temperature changes. The Zerodur mirror was constructed using Schott's standard process, so the test results are indicative of what to expect from future Zerodur mirrors.

REFERENCES

[1] Hadaway, James B., et al, "Cryogenic performance of lightweight SiC and C/SiC mirrors", *Proc SPIE* 5487, Optical, Infrared, and Millimeter Space Telescopes, (12 October 2004); doi: 10.1117/552409; https://doi.org/10.1117/12.552409

[2] Schott, "ZERODUR ® Zero Expansion Glass Ceramic," Schott website, July 2011, http://www.schott.com/d/advanced_optics/f7ae3c11-0226-4808-90c7-59d6c8816daf/1.0/schott_zerodur_katalog_july_2011_en.pdf (July 2011).

[3] Jedamzik, Ralf, et al., "Effects of thermal inhomogeneity on 4m class mirror substrates", *Proc. SPIE* 9912, Advances in Optical and Mechanical Technologies for Telescopes and Instrumentation II, 99120Z (July 22, 2016); doi:10.1117/12.2234287; http://dx.doi.org/10.1117/12.2234287

[4] Brooks, Thomas E., et al., "Modeling the Extremely Lightweight Zerodur Mirror (ELZM) thermal soak test", *Proc. SPIE* 10374, Optical Modeling and Performance Predictions IX, 103740E (6 September 2017); doi: 10.1117/12.2274084; http://dx.doi.org/10.1117/12.2274084